Superlattices and Microstructures xxx (2017) 1–8

Contents lists available at ScienceDirect

Superlattices and Microstructures

journal homepage: www.elsevier.com/locate/superlattices

# Transport through a non-Hermitian parallel double-quantum-dot structure in the presence of interdot Coulomb interaction

Lian-Lian Zhang, Guo-Hui Zhan, Dian-Qiang Yu, Wei-Jiang Gong*

*College of Sciences, Northeastern University, Shenyang 110819, China*

ARTICLE INFO

*Article history:*
Received 20 July 2017
Received in revised form 20 November 2017
Accepted 21 November 2017
Available online xxx

*Keywords:*
Double quantum dot
$\mathscr{PT}$-symmetric complex potentials
Transport property
Interdot Coulomb interaction

ABSTRACT

In this work, we investigate the effect of $\mathscr{PT}$-symmetric complex potentials on the transport properties of one non-Hermitian system, which is formed by a parallel coupled double-quantum-dot geometry. It is found that the $\mathscr{PT}$-symmetric complex potentials take pronounced effects to the transport properties of such a system, manifested as the occurrence of antiresonance. In the presence of the interdot Coulomb interaction, such potentials lead to the shift and increase of the antiresonance points, dependent on the Coulomb interaction strength. This study exhibits the special impact of the interplay between the interdot Coulomb interaction and $\mathscr{PT}$-symmetric potentials on the quantum transport behaviors.



## 1. Introduction

During the past two decades, much attention in both theoretical analysis and experimental investigation have been given to developing the discovery of non-Hermitian Hamiltonians with parity-time($\mathscr{PT}$) symmetry, due to the real energy spectra of them [1]. Motivated by the experimental reports, scientists make efforts to establish the $\mathscr{PT}$-symmetric quantum theory as a complex extension of the conventional quantum mechanics [2–7]. Meanwhile, numerous $\mathscr{PT}$-symmetric systems have been explored, such as open quantum systems [8], the optical systems with complex refractive indices [9–13], the Anderson models for disorder systems [14–16] and the topological insulators [17,18]. Recently, Rüter and colleagues demonstrated that a new class of synthetic materials called $\mathscr{PT}$ materials can exhibit intriguing properties, such as the power oscillations, the non-reciprocal light propagation and the tailed energy flow [19]. These results have stimulated a lot of the following experimental researches [20–28].

The theoretical and experimental progresses inspire researchers to focus further studies on the non-Hermitian lattice models with ($\mathscr{PT}$)-symmetry [29–34]. The other reason consists in that the $\mathscr{PT}$-symmetric systems have the tractable numerical and analytical calculations with the available exact solutions. As a result, the physics properties of the $\mathscr{PT}$-symmetric systems of non-Hermitian Hamiltonians have also become one significant concern in quantum systems on account of more and more exploration and fabrication in this field. In Ref. [35], a $\mathscr{PT}$-symmetric ring lattice, with one pair of balanced gain and loss located at opposite positions, is sensitive to the magnetic flux, and the maximally tolerable magnetic flux for the exact $\mathscr{PT}$-symmetric phase has also been observed.

* Corresponding author.
*E-mail address:* gwj@mail.neu.edu.cn (W.-J. Gong).

https://doi.org/10.1016/j.spmi.2017.11.040
0749-6036/

Recent studies showed that the $\mathscr{PT}$-symmetric imaginary potentials can lead to some pronounced effects on transport properties in some low-dimensional systems. For one Fano-Anderson system, they give rise to the changes from the perfect reflection to perfect transmission, as well as the behaviors for the absence or existence of the perfect reflection at one and two resonant frequencies [36]. In a non-Hermitian Aharonov-Bohm ring with one quantum dot(QD) embedded in each of its two arms, the asymmetric Fano profile will show up in the conductance spectrum just by non-Hermitian quantity in this system, by the presence of appropriate parameters [37]. Other studies have reported that in the rhombic QD ring, the nonreciprocal phase shifts induced by the magnetic flux and gain/loss break $\mathscr{P}$ and $\mathscr{T}$ symmetry but keep the $\mathscr{PT}$ symmetry. Meanwhile, the reciprocal reflection(transmission) and unidirectional transmission(reflection) appear in the axial(reflection) $\mathscr{PT}$-symmetric ring center [38]. As thus, one can ascertain that in the $\mathscr{PT}$-symmetric systems of non-Hermitian Hamiltonians, the $\mathscr{PT}$-symmetric imaginary potentials play nontrivial roles in modulating the quantum interference that governs the quantum transport process. Almost surely, some other typical geometries should be investigated for further understanding the role of $\mathscr{PT}$-symmetric imaginary potentials in modifying the transport properties in low-dimensional systems.

It is well known that QDs are characterized by the Coulomb interaction due to the spatial confinement of electrons in them. So many previous works have demonstrated that the strong Coulomb interaction gives rise to the level hybridization of the QD molecule, which brings about novel transport phenomena, such as the two-group transport spectra and the Kondo effect [39]. In comparison with the intradot electron interaction, the interdot Coulomb repulsion is a special mechanism to affect the quantum transport through QD systems [40]. For instance, it can induce the orbital-Kondo effect, which shows high adjustability following the change of the structural parameters or external fields [41–43].

All of above enlighten us on discussing the $\mathscr{PT}$ symmetry and Coulomb interaction in a new study direction. In the present work, we would like to study the effect of interdot Coulomb interaction on the transport behaviors induced by the $\mathscr{PT}$-symmetric complex potentials in non-Hermitian systems. Following this idea, we construct one parallel coupled double-QD structure, and then introduce the $\mathscr{PT}$-symmetric complex potentials to the QDs. The calculation results show that the $\mathscr{PT}$-symmetric imaginary potentials take pronounced effects to the transport properties of such a system, accompanied by the occurrence of antiresonance. Next, when the interdot Coulomb interaction is taken into account, the antiresonance effect is modified to a great extent, including the shift and increase of the antiresonance points.

## 2. Theoretical model

The parallel-coupled double-QD structure that we consider is illustrated in Fig. 1. The Hamiltonian to describe the electron motion in this system reads

$$H = H_C + H_D + H_T. \tag{1}$$

The first term is the Hamiltonian for the noninteracting electrons in the two leads:

$$H_C = \sum_{k\alpha\in L,R} \varepsilon_{\alpha k} c^{\dagger}_{\alpha k} c_{\alpha k}, \tag{2}$$

where $c^{\dagger}_{\alpha k}$ ($c_{\alpha k}$) is an operator to create (annihilate) an electron of the continuous state $k$ in lead-$\alpha$, and $\varepsilon_{\alpha k}$ is the corresponding single-particle energy. The second term describes the electron in the double QDs. It takes a form as

$$H_D = \sum_{j=1}^{2} \varepsilon_j d^{\dagger}_j d_j + U n_1 n_2 + t_c d^{\dagger}_1 d_2 + h.c., \tag{3}$$

where $d^{\dagger}_j$ ($d_j$) is the creation (annihilation) operator of electron in QD-$j$, and $\varepsilon_j$ denotes the electron level in the corresponding QD. $U$ represents the interdot Coulomb interaction strength, and $t_c$ describes the interdot coupling. We assume that only one level is relevant in each QD, since we are only interested in the effects of interdot Coulomb interaction and $\mathscr{PT}$-symmetric potentials. The last term in the Hamiltonian denotes the electron tunnelling between the leads and QDs. It is given by

$$H_T = \sum_{k\alpha j} \left( V_{j\alpha} d^{\dagger}_j c_{\alpha k} + h.c. \right), \tag{4}$$

where $V_{j\alpha}$ denotes the QD-lead coupling coefficient. In our considered geometry, the effect of the $\mathscr{P}$ operator is to let $\mathscr{P} d_1 \mathscr{P} = d_2$ with the linear chain as the mirror axis, and the effect of the $\mathscr{T}$ operator is $\mathscr{T} i \mathscr{T} = -i$. Thus, it is not difficult to find that the Hamiltonian is invariant under the combined operation $\mathscr{PT}$, under the condition of $E_1 = E_2^*$ for the case of uniform QD-lead coupling.

To study the electron-transport properties, we would like to adopt the nonequilibrium Green-function technique [44,45]. However, due to the presence of interdot Coulomb interaction, the Green function cannot be strictly solved. Thus, the approximation method should be introduced, whose feasibility is determined by the Coulomb strength.

Please cite this article in press as: L.-L. Zhang et al., Transport through a non-Hermitian parallel double-quantum-dot structure in the presence of interdot Coulomb interaction, Superlattices and Microstructures (2017), https://doi.org/10.1016/j.spmi.2017.11.040

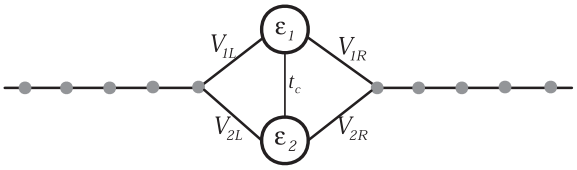


**Fig. 1.** Schematic of one non-Hermitian double-QD circuit. The QDs are influenced by $\mathscr{PT}$-symmetric complex on-site chemical potentials. In this system, only one level is considered to be in each QD. The QD-lead coupling coefficients are defined by $V_{j\alpha}$, and the interdot coupling is denoted as $t_c$.

For the cases of weak or mediate Coulomb interaction, the Hartree-Fock or Hubbard-I approximations can be suitable to achieve the solution [46]. In such cases, the transmission function is given as

$$T(\omega) = 4\mathrm{Tr}\left[\Gamma^L G^r \Gamma^R G^a\right], \tag{5}$$

which is identical with the noninteracting case. $\Gamma^L$ is a $2 \times 2$ matrix, describing the coupling strength between the two QDs and the left lead. It is defined as $[\Gamma^L]_{jn} = \pi V_{jL} V_{Ln} \rho_0(\omega)$ ($V_{Ln} = V_{nL}^*$). We can ignore the $\omega$-dependence of $\Gamma_{jn}^L$ since the electron density of states $\rho_0(\omega)$ can be viewed as a constant at the wide-band limit. By the same token, we can define $[\Gamma^R]_{jn}$. In Eq. (5) the retarded and advanced Green functions in Fourier space are involved. Meanwhile, the Green functions are defined as follows: $G_{jl}^r(t) = -i\theta(t)\langle\{d_j(t), d_l^\dagger\}\rangle$ and $G_{jl}^a(t) = i\theta(-t)\langle\{d_j(t), d_l^\dagger\}\rangle$, where $\theta(x)$ is the step function. The Fourier transforms of the Green functions can be performed via $G_{jl}^{r(a)}(\omega) = \int_{-\infty}^{\infty} G_{jl}^{r(a)}(t) e^{i\omega t} dt$. These Green functions can be solved by means of the equation-of-motion method. We introduce an alternative notation $\langle\langle A|B\rangle\rangle^x$ with $x = r$ or $a$ to denote the Green functions in Fourier space, e.g., $G_{jl}^r(\omega)$ is identical to $\langle\langle d_j \middle| d_l^\dagger \rangle\rangle^r$. The Green functions obey the following equation of motion

$$\left(\omega \pm i0^+\right)\langle\langle A|B\rangle\rangle^{r(a)} = \langle\{A, B\}\rangle + \langle\langle [A, H]|B\rangle\rangle^{r(a)}. \tag{6}$$

Starting from Eq. (6), we can first derive the equation of motion of the retarded Green function $\langle\langle d_{j\sigma} \middle| d_{l\sigma}^\dagger \rangle\rangle^r$ between two arbitrary QDs in the main chain, which yields

$$\begin{aligned}
&(\omega - \varepsilon_1 + i\Gamma_{11})\langle\langle d_1 \middle| d_l^\dagger \rangle\rangle^r \\
&= \delta_{1l} + (t_c - i\Gamma_{12})\langle\langle d_2 \middle| d_l^\dagger \rangle\rangle^r + U\langle\langle d_1 n_2 \middle| d_l^\dagger \rangle\rangle^r, \\
&(\omega - \varepsilon_2 + i\Gamma_{22})\langle\langle d_2 \middle| d_l^\dagger \rangle\rangle^r \\
&= \delta_{2l} + (t_c - i\Gamma_{21})\langle\langle d_1 \middle| d_l^\dagger \rangle\rangle^r + U\langle\langle d_2 n_1 \middle| d_l^\dagger \rangle\rangle^r.
\end{aligned} \tag{7}$$

In the above equations, $\Gamma_{jl} = \Gamma_{jl}^L + \Gamma_{jl}^R$. Besides, the many-body terms are involved, we have to truncate the equations of motion at some order to form a closed set of equations. The roughest approach is the Hartree-Fock approximation, which means that $\langle\langle d_j n_{j'} \middle| d_l^\dagger \rangle\rangle^r \approx \langle n_{j'} \rangle \langle\langle d_j \middle| d_l^\dagger \rangle\rangle^r$ is adopted to deal with these Green functions associated with the many-body terms. Beyond the Hartree-Fock approximation, we arrive at the Hubbard-I approximation, which is to truncate the equations of motion of the Green functions $\langle\langle d_j n_{j'} \middle| d_l^\dagger \rangle\rangle^r$ in the following way:

$$\begin{aligned}
&(z - \varepsilon_1 - U)\langle\langle d_1 n_2 \middle| d_l^\dagger \rangle\rangle^r \\
&= \langle n_2 \rangle \delta_{1l} + (t_c - i\Gamma_{12})(1 - \delta_{j2})\langle n_2 \rangle \langle\langle d_1 \middle| d_l^\dagger \rangle\rangle^r, \\
&(z - \varepsilon_2 - U)\langle\langle d_2 n_1 \middle| d_l^\dagger \rangle\rangle^r \\
&= \langle n_1 \rangle \delta_{2l} + (t_c^* - i\Gamma_{21})(1 - \delta_{j1})\langle n_1 \rangle \langle\langle d_2 \middle| d_l^\dagger \rangle\rangle^r.
\end{aligned} \tag{8}$$

Following this equation and by a straightforward derivation, we obtain the retarded Green functions which are written in a matrix form as

Please cite this article in press as: L.-L. Zhang et al., Transport through a non-Hermitian parallel double-quantum-dot structure in the presence of interdot Coulomb interaction, Superlattices and Microstructures (2017), https://doi.org/10.1016/j.spmi.2017.11.040

$$G^r(\omega) = \begin{bmatrix} g_1(\omega)^{-1} & -t_c + i\Gamma_{12} \\ -t_c^* + i\Gamma_{21} & g_2(\omega)^{-1} \end{bmatrix}^{-1}. \tag{9}$$

here $g_j = [(\omega - \varepsilon_j)S_j + i\Gamma_{jj}]^{-1}$ with $S_j(\omega) = \frac{z-\varepsilon_j-U}{z-\varepsilon_j-U+U\langle n_{j'}\rangle}$, where the average electron occupation numbers in QDs are determined by the relations $\langle n_j\rangle = \int d\omega \left[-\frac{1}{\pi}\mathrm{Im}G^r_{jj}(\omega)\right] f(\omega).f(\omega) = \left[\exp\frac{\omega-\mu}{k_BT}+1\right]^{-1}$ is the Fermi distribution, and it is simplified to be one theta function at the zero-temperature case.

Surely, with the help of above derivation, one can write out the expression of the transmission function. However, due to its complication, we would like to present the transmission coefficient which is defined by $\tau_t = \sum_{jl} \tilde{V}_{Lj} G_{jl} \tilde{V}_{jR}$ with $\tilde{V}_{\alpha j} = V_{\alpha j}\sqrt{\rho_0}$:

$$\tau_t = 2\frac{\left[\sqrt{\Gamma^L_{22}\Gamma^R_{22}}\,(\omega-\varepsilon_1)S_1 + \sqrt{\Gamma^L_{11}\Gamma^R_{11}}\,(\omega-\varepsilon_2)S_2 + t_c\sqrt{\Gamma^L_{11}\Gamma^R_{22}} + t_c^*\sqrt{\Gamma^L_{22}\Gamma^R_{11}}\right]}{\prod_{j=1}^2[(\omega-\varepsilon_j)S_j + i\Gamma_{jj}] - (t_c - i\Gamma_{12})(t_c^* - i\Gamma_{21})}. \tag{10}$$

Under the situation of $\Gamma^\alpha_{jj} = \Gamma_0$ and $\varepsilon_{1(2)} = \varepsilon \mp i\gamma$, $\tau_t$ will be simplified as

$$\tau_t = \frac{\Gamma_0[(S_1+S_2)(\omega-\varepsilon) + 2t_c + i\gamma(S_2-S_1)]}{S_1S_2\left[(\omega-\varepsilon)^2+\gamma^2\right] - t_c^2 + \gamma\Gamma_0(S_1-S_2) + i\Gamma_0[2t_c + (S_1+S_2)(\omega-\varepsilon)]}, \tag{11}$$

with the real $t_c$.

For the case of weak Coulomb interaction, we can handle the many-body term within the Hartree-Fock approximation. In such a case, $g_j$ has the same form with the zero-Coulomb result, except that $\varepsilon_j$ should be changed to $\varepsilon_j + U\langle n_{j'}\rangle$.

## 3. Numerical results and discussions

With the formulation developed in Sec. 2, we can perform the numerical calculation to investigate the transmission function spectrum of our considered parallel double-QD structure. Prior to calculation, we would like to emphasize the parameter order. According to the QD-related experiments, the parameter order can be assumed to be *meV*[47].

First of all, we present the transmission function property in the absence of interdot Coulomb interaction. Without loss of generality, we take the parameter values as $t_c = 0.1$ and $\Gamma_0 = 0.5$ to perform the numerical calculation, and the corresponding results are shown in Fig. 2(a) and (b). It is clearly found that in the absence of $\mathscr{PT}$-symmetric complex potentials, the transmission function spectrum only shows one peak in the vicinity of $\omega = \varepsilon$. This result is exactly caused by the occurrence of the decoupling mechanism, and it can be analyzed as follows. For the double QDs, the unitary matrix that describes the "atomic" and "molecular" states takes a form as $[\boldsymbol{\eta}] = \frac{1}{\sqrt{2}}\begin{bmatrix} -1 & 1 \\ 1 & 1 \end{bmatrix}$, and the molecular levels are $E_{1(2)} = \varepsilon \pm t_c$, respectively. One can then know that the coupling between the bonding state and lead-$\alpha$, related to $[\boldsymbol{\eta}]^\dagger_{11} + [\boldsymbol{\eta}]^\dagger_{21}$, is equal to zero, so the bonding state decouples from the leads completely. Next, we introduce the $\mathscr{PT}$-symmetric complex potentials to the two QDs, by considering $\varepsilon_1 = \varepsilon - i\gamma$ and $\varepsilon_2 = \varepsilon + i\gamma$. The results in Fig. 2(a) and (b) show that the nonzero $\gamma$ leads to the disappearance of the decoupling phenomenon. Meanwhile, a distinct antiresonance point appears in the transmission function spectra. The increase of $\gamma$ only widens the antiresonance valley and suppresses the spectrum magnitude but cannot change the antiresonance position.

These results can be understood by writing out the analytical expression of the transmission function. After one straightforward deduction, we get the result that

$$T(\omega) = \frac{4\Gamma_0^2(\omega-\varepsilon+t_c)^2}{\left[(\omega-\varepsilon)^2+\gamma^2-t_c^2\right]^2 + 4\Gamma_0^2(\omega-\varepsilon+t_c)^2}. \tag{12}$$

It clearly shows that in the case of $\gamma = 0$, the transmission function is simplified as $T(\omega) = \frac{4\Gamma_0^2}{(\omega-\varepsilon-t_c)^2+4\Gamma_0^2}$, whose profile shows up as a Breit-Wigner lineshape. Next, the presence of $\mathscr{PT}$-symmetric complex potentials leads to the disappearance of decoupling mechanism, and induces the occurrence of antiresonance phenomenon. In addition, we can find that in the case of nonzero $\gamma$, $[\boldsymbol{\eta}] = \frac{1}{\sqrt{2\cos\theta}}\begin{bmatrix} -e^{i\theta} & e^{-i\theta} \\ 1 & 1 \end{bmatrix}$ with $\theta = \arctan\frac{\gamma}{t_c}$. Surely, it is the change of the phase and magnitude of the transmission paths that induces the antiresonance effect.

Please cite this article in press as: L.-L. Zhang et al., Transport through a non-Hermitian parallel double-quantum-dot structure in the presence of interdot Coulomb interaction, Superlattices and Microstructures (2017), https://doi.org/10.1016/j.spmi.2017.11.040

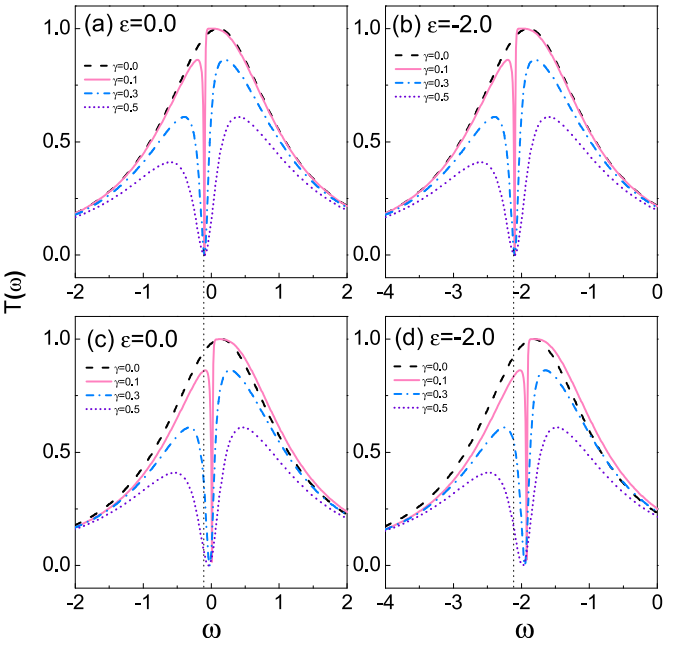


**Fig. 2.** Spectra of the transmission function of the parallel coupled double-QD system influenced by the $\mathscr{PT}$-symmetric complex potentials. The structure parameters are taken to be $t_c = 0.1$ and $\Gamma_0 = 0.5$. (a)–(b) Transmission-function spectra in the noninteracting case. (c)–(d) Results of weak interdot Coulomb interaction with $U = 0.2$. (For interpretation of the references to colour in this figure legend, the reader is referred to the web version of this article.)

Following the noninteracting results, we take the interdot Coulomb interaction into account, to investigate its impact on the transmission function property. In the case of weak Coulomb interaction, the Coulomb term can be managed within the Hartree-Fock approximation. The results are shown in Fig. 2(c) and (d), where the Coulomb strength is taken to be $U = 0.2$. In these two figures, it can be found that the transmission function spectra are basically similar to those in the noninteracting case, regardless of the absence or presence of the $\mathscr{PT}$-symmetric complex potentials. The only difference consists that the Coulomb interaction causes the transmission function spectra to shift to the high-energy direction. Such a result should be attributed to the addition of the QD levels within the Hartree-Fock approximation, i.e., $\varepsilon_j \rightarrow \varepsilon_j + U\langle n_{\bar{j}}\rangle$. Note that since the average electron number in the QD is determined by the structural parameter of the whole system, the antiresonance point experiences a weak right shift in such a case.

Next, we increase the interdot Coulomb strength to further present the transmission function spectra modified by the $\mathscr{PT}$-symmetric complex potentials. The results are exhibited in Figs. 3–5, where the Coulomb strength is taken to be $U = 0.5$, 1.0, 2.0, and 3.0, respectively. Due to the increased Coulomb strength, we handle the interdot electron interaction within the Hubbard-I approximation in these cases. In Fig. 3, one can find that in the absence of $\mathscr{PT}$-symmetric complex potentials, the interdot Coulomb interaction causes the transmission function spectra to split into two groups, with an antiresonance point in between. The reason should be attributed to the Coulomb-induced level splitting within the Hubbard-I approximation. When the $\mathscr{PT}$-symmetric complex potentials are introduced, i.e., $\gamma \neq 0$, the results are complicated, which are also dependent on the QD levels. To be concrete, in the case of $\varepsilon = 0$, it shows that when $\gamma = 0.1$, one antiresonance point emerges beside the original one. Meanwhile, a new dip appears near the energy zero point. With the increase of $\gamma$, such a dip transits into an antiresonance point and its valley is widened gradually. In contrast, the other antiresonances vanish. For the case of $\varepsilon = -0.5$, in Fig. 3(b) we see that while $\gamma = 0.1$, its-induced antiresonance points get close to each other, with the consistency of the two antiresonance valleys. And then, the increase of $\gamma$ enhances the antiresonance result. Next, if the QD levels shift to the position $\varepsilon = -1.0$, the complex potentials can only induce one antiresonance even in the case of $\gamma = 0.1$. As $\gamma$ increases, only one antiresonance can be observed in the transmission function spectrum, similar to the results in Fig. 3(a) and (b). However, Fig. 3(d) shows that the $\mathscr{PT}$-symmetric complex potentials have an opportunity to suppress the antiresonance. As shown by the result of $\gamma = 0.1$, only two dips appear in the transmission function profile, but they are obviously greater than zero. In Fig. 3, it shows that when $\gamma = 0.1$, the maximum of transmission peaks equals 1.0 and the peaks on the left side of the antiresonance point are suppressed with $\varepsilon < 0$.

In Fig. 4, we increase the interdot Coulomb interaction to $U = 1.0$ to investigate the change of the transmission function. It is firstly found that in the absence of $\mathscr{PT}$-symmetric complex potentials, the interdot Coulomb interaction causes the transmission function spectra to split into two groups, with the widened antiresonance valley in between. When the $\mathscr{PT}$-symmetric complex potentials are incorporated, their effects are more complicated compared with the case of $U = 0.5$. In the case of $\gamma = 0.1$, such potentials move the Coulomb-induced antiresonance to the low-energy direction, and they introduce new antiresonance in each group of the transmission function spectra. Meanwhile, the two groups become more

Please cite this article in press as: L.-L. Zhang et al., Transport through a non-Hermitian parallel double-quantum-dot structure in the presence of interdot Coulomb interaction, Superlattices and Microstructures (2017), https://doi.org/10.1016/j.spmi.2017.11.040

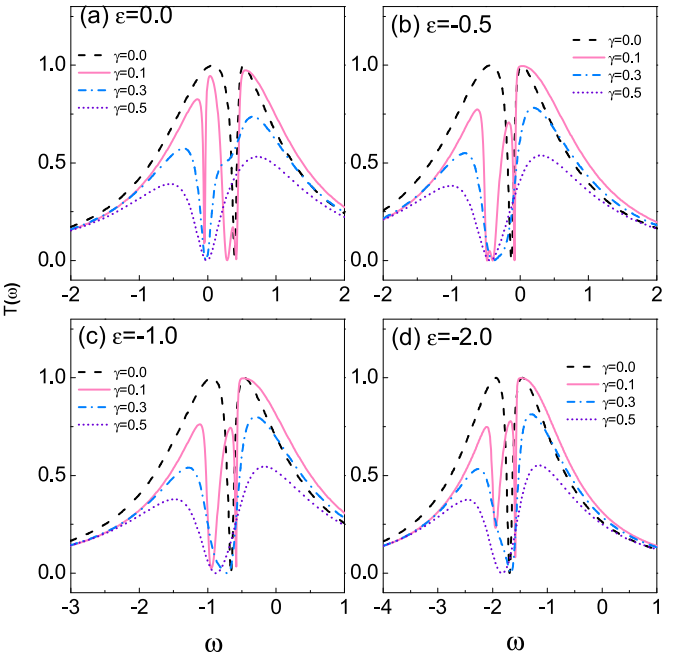


**Fig. 3.** Transmission-function spectra of the parallel coupled double-QD system modified by the $\mathscr{PT}$-symmetric complex potentials, when the interdot Coulomb interaction is taken to be $U = 0.5$. Relevant structure parameters are $t_c = 0.1$ and $\Gamma_0 = 0.5$. (For interpretation of the references to colour in this figure legend, the reader is referred to the web version of this article.)

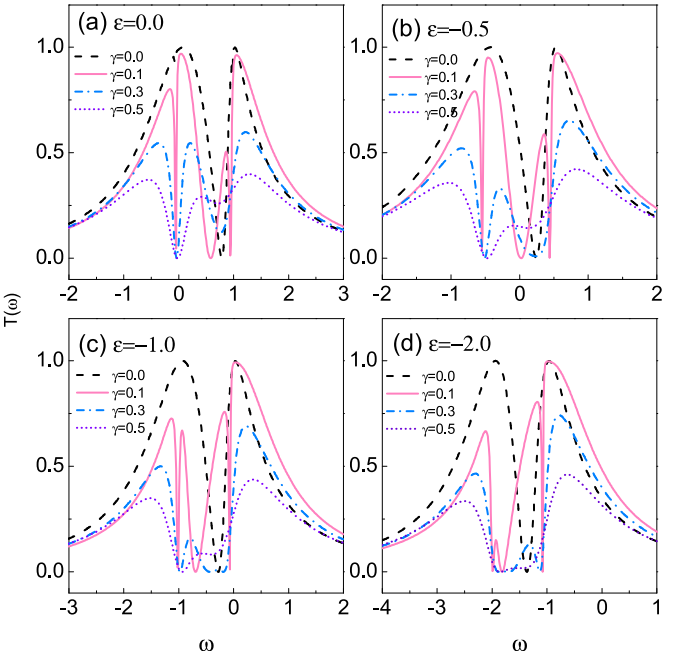


**Fig. 4.** Transmission-function spectra of the parallel coupled double-QD system, when the interdot Coulomb interaction $U = 1.0$. Relevant structure parameters are the same as those in Fig. 3. (For interpretation of the references to colour in this figure legend, the reader is referred to the web version of this article.)

different from each other. When $\gamma$ increase to 0.3, the two-group profile of the transmission function disappears, and the number of antiresonance points decreases, in the cases of $\varepsilon = 0$ and $\varepsilon = -0.5$. Especially for $\varepsilon = 0$, only one antiresonance can be observed at the energy zero point. Contrarily, the antiresonance result is still apparent in the cases of $\varepsilon = -1.0$ and $\varepsilon = -2.0$. Next, when $\gamma$ further increases, the oscillation of the transmission function spectra becomes weak, accompanied by one antiresonance point, regardless of the values of QD levels.

Please cite this article in press as: L.-L. Zhang et al., Transport through a non-Hermitian parallel double-quantum-dot structure in the presence of interdot Coulomb interaction, Superlattices and Microstructures (2017), https://doi.org/10.1016/j.spmi.2017.11.040

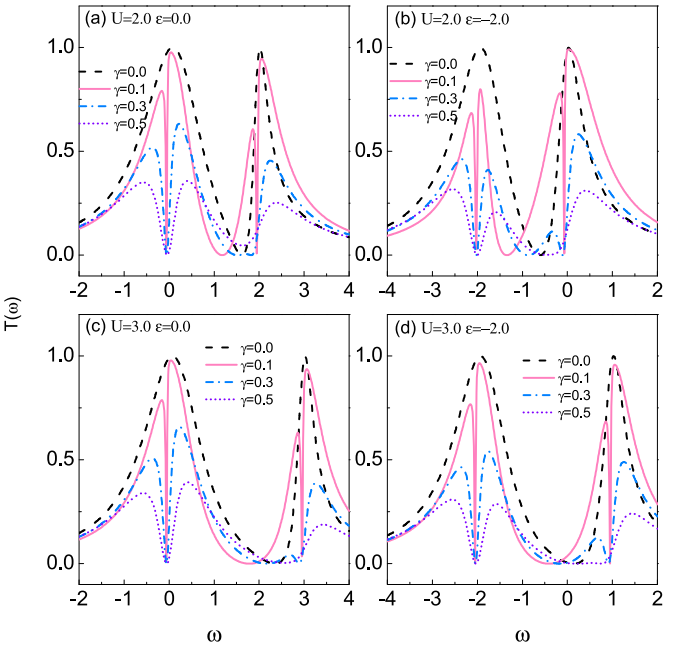


**Fig. 5.** Transmission-function spectra of the parallel coupled double-QD system, in the cases of $U = 2.0$ and $U = 3.0$. Structure parameters are the same as those in Fig. 3. (For interpretation of the references to colour in this figure legend, the reader is referred to the web version of this article.)

The results in Figs. 3–4 suggest that the increase of Coulomb interaction changes the hybridization of the levels of QD molecule, which modifies the quantum transport behaviors induced by the $\mathscr{PT}$-symmetric complex potentials. Therefore, we would like to going on enhancing the Coulomb interaction to clarify how the interplay between the interdot Coulomb interaction and $\mathscr{PT}$-symmetric potentials to contributes to the quantum transport through this system. In Fig. 5, we plot the transmission function spectra of $U = 2.0$ and $U = 3.0$. It can be seen that in such a case, the Coulomb interaction enlarges the distance of the two groups of the transmission function spectra. As for effects of the $\mathscr{PT}$-symmetric complex potentials, they move the Coulomb-induced antiresonance to the low-energy direction, and they introduce new antiresonance in each group of the transmission function spectra. These results can be observed in the case of $\gamma = 0.1$. When $\gamma = 0.3$, the left peak of the high-energy group in the transmission function spectrum is seriously suppressed, especially in the case of $\varepsilon = 0$. This changes the two-group profile of the transmission function. However, the antiresonance point in the high-energy group still exists in such a case. Next, in the case of $\gamma = 0.5$, such an antiresonance point is eliminated. With respect to the antiresonance in the low-energy group of the transmission function spectrum, it is robust and consistent with the value of QD level.

Up to now, we have understood that in the presence of interdot Coulomb interaction, the effects of the $\mathscr{PT}$-symmetric complex potentials become more complicated, the increase, shift, or decrease of the antiresonance points and the modification of the transmission function spectra. All these results are determined by the interplay between the potential strength $\gamma$ and the structural parameters.

## 4. Summary

To summarize, in this work we have discussed the effect of $\mathscr{PT}$-symmetric complex potentials on the transport properties of one non-Hermitian system, which is formed by the parallel coupling between a double-QD molecule and two normal metallic leads. As a result, it has been found that the $\mathscr{PT}$-symmetric imaginary potentials take pronounced effects to the transport properties of such a system, accompanied by the occurrence of antiresonance. In the following, when the interdot Coulomb interaction is taken into account, the effects of such $\mathscr{PT}$-symmetric complex potentials become more intricate, including the increase and shift of the antiresonance points. We believe that the results in this work can assist to understand the special role of the interdot Coulomb interaction in modulating the quantum transport behaviors modified by the $\mathscr{PT}$ symmetry in non-Hermitian systems.

## References

[1] C.M. Bender, S. Boettcher, Phys. Rev. Lett. 80 (1998) 5243.
[2] C.M. Bender, D.C. Brody, H.F. Jones, Phys. Rev. Lett. 89 (2002) 270401.
[3] A. Mostafazadeh, J. Math. Phys. 43 (2002) 205 ibid 43, 2814(2002).
[4] C.M. Bender, D.C. Brody, H.F. Jones, Phys. Rev. D. 70 (2004) 025001;
a H.F. Jones, J. Phys. A 39 (2006) 10123.

Please cite this article in press as: L.-L. Zhang et al., Transport through a non-Hermitian parallel double-quantum-dot structure in the presence of interdot Coulomb interaction, Superlattices and Microstructures (2017), https://doi.org/10.1016/j.spmi.2017.11.040

[5] I. Rotter, J. Phys. A 42 (2009) 153001.
[6] I.Y. Goldsheid, B.A. Khoruzhenko, Phys. Rev. Lett. 80 (1998) 2897.
[7] J. Heinrichs, Phys. Rev. B 63 (2001) 165108.
[8] L.G. Molinari, J. Phys. A 42 (2009) 265204.
[9] S. Klaiman, U. Günther, N. Moiseyev, Phys. Rev. Lett. 101 (2008) 080402;
a K.G. Makris, R. El-Ganainy, D.N. Christodoulides, Z.H. Musslimani, Phys. Rev. Lett. 100 (2008) 103904;
[10] A.A. Sukhorukov, Z. Xu, Y.S. Kivshar, Phys. Rev. A 82 (2010) 043818.
[11] H. Ramezani, D.N. Christodoulides, V. Kovanis, I. Vitebskiy, T. Kottos, Phys. Rev. Lett. 109 (2012) 033902.
[12] Z.H. Musslimani, K.G. Makris, R. El-Ganainy, D.N. Christodoulides, Phys. Rev. Lett. 100 (2008) 030402.
[13] X.B. Luo, J.H. Huang, H.H. Zhong, X.Z. Qin, Q.T. Xie, Y.S. Kivshar, C.H. Lee, Phys. Rev. Lett. 110 (2013) 243902.
[14] Y.C. Hu, T.L. Hughes, Phys. Rev. B 84 (2011) 153101;
[15] B.G. Zhu, R. Lü, S. Chen, Phys. Rev. A 89 (2014) 062102.
[16] A. Guo, G.J. Salamo, D. Duchesne, R. Morandotti, M. Volatier-Ravat, V. Aimez, G.A. Siviloglou, D.N. Christodoulides, Phys. Rev. Lett. 103 (2009) 093902.
[17] C.E. Rüter, K.G. Makris, R. El-Ganainy, D.N. Christodoulides, M. Segev, D. Kip, Nat. Phys. 6 (2010) 192.
[18] A. Regensburger, M.A. Miri, C. Bersch, J. Näger, G. Onishchukov, D.N. Christodoulides, U. Peschel, Phys. Rev. Lett. 110 (2013) 223902.
[19] A. Regensburger, C. Bersch, M.A. Miri, G. Onishchukov, D.N. Christodoulides, U. Peschel, Nature 488 (2010) 166.
[20] J. Schindler, A. Li, M.C. Zheng, F.M. Ellis, T. Kottos, Phys. Rev. A 84 (2011) 040101(R).
[21] M. Znojil, Phys. Rev. A 82 (2010) 052113.
[22] O. Bendix, R. Fleischmann, T. Kottos, B. Shapiro, Phys. Rev. Lett. 103 (2009) 030402.
[23] L. Chang, X.S. Jiang, S.Y. Huai, C. Yang, J.M. Wen, L. Jiang, G.Y. Li, G.Z. Wang, M. Xiao, Nat. Photonics 8 (2014) 524.
[24] B. Peng, S.K. Ozdemir, F. Lei, F. Monifi, M. Gianfreda, G.L. Long, S. Fan, F. Nori, C.M. Bender, L. Yang, Nat. Phys. 10 (2014) 394.
[25] R. Fleury, D. Sounals, A. Alu, Nat. Commun. 6 (2015) 5905.
[26] M. Wimmer, A. Regensburger, M.A. Miri, C. Bersch, D.N. Christodoulides, U. Peschel, Nat. Commun. 6 (2015) 7782.
[27] L. Feng, Z.J. Wong, R.M. Ma, Y. Wang, X. Zhang, Science 346 (2014) 972.
[28] C. Hahn, Y. Choi, J.W. Yoon, S.H. Song, C.H. Oh, P. Berini, Nat. Commun. 7 (2016) 12201.
[29] L. Jin, Z. Song, Phys. Rev. A 80 (2009) 052107;
a W.H. Hu, L. Jin, Y. Li, Z. Song, Phys. Rev. A 86 (2012) 042110.
[30] Y.N. Joglekar, A. Saxena, Phys. Rev. A 83 (2011) 050101(R).
[31] G.D. DellaValle, S. Longhi, Phys. Rev. A 87 (2013) 022119;
a F. Tellander, K.F. Berggren, Phys. Rev. A 95 (2017) 042115.
[32] L. Jin, Z. Song, Phys. Rev. A 85 (2012) 012111.
[33] B.P. Nguyen, K. Kim, Phys. Rev. A 94 (2016) 062122;
a L. Praxmeyer, P. Yang, R.K. Lee, Phys. Rev. A 93 (2016) 042122.
[34] C.M. Bender, N. Hassanpour, D.W. Hook, S.P. Klevansky, C. Sünderhauf, Z. Wen, Phys. Rev. A 95 (2017) 052113;
a M. Klett, H. Cartarius, D. Dast, J. Main, G. Wunner, Phys. Rev. A 95 (2017) 053626.
[35] L. Jin, Z. Song, Phys. Rev. A 93 (2016) 062110.
[36] B. Zhu, R. Lü, S. Chen, Phys. Rev. A 91 (2015) 042131.
[37] Q. B. Zeng, S. Chen, and R. Lü, arXiv: 1608.00065v2.
[38] L. Jin, X.Z. Zhang, G. Zhang, Z. Song, Sci. Rep. 6 (2016) 20976.
[39] P. Trocha, J. Barnaś, Phys. Rev. B 76 (2007) 165432;
a R. López, D. Sánchez, L. Serra, Phys. Rev. B 76 (2007) 035307.
[40] R. López, D. Sánchez, M. Lee, M.S. Choi, P. Simon, K.L. LeHur, Phys. Rev. B 71 (2005) 115312.
[41] D. Feinberg, P. Simon, Appl. Phys. Lett. 85 (2004) 1846;
a A. Hübel, K. Held, J. Weis, K. v. Klitzing, Phys. Rev. Lett. 101 (2008) 186804;
b C.A. Büsser, A.E. Feiguin, G.B. Martins, Phys. Rev. B 85 (2012) 241310(R).
[42] S. Sasaki, S. Amaha, N. Asakawa, M. Eto, S. Tarucha, Phys. Rev. Lett. 93 (2004) 017205;
a P.G. Silvestrov, Y. Imry, Phys. Rev. B 75 (2007) 115335;
b P. Trocha, Phys. Rev. B 82 (2010) 125323;
c Y. Okazaki, S. Sasaki, K. Muraki, Phys. Rev. B 84 (2011) 161305(R);
d L. Tosi, P. Roura-Bas, A.A. Aligia, Phys. Rev. B 88 (2013) 235427;
e Y. Komijani, P. Simon, I. Affleck, Phys. Rev. B 92 (2015) 075301;
f Y. Nishida, Phys. Rev. A 93 (2016) 011606(R);
g A. Wong, A.T. Ngo, S.E. Ulloa, Phys. Rev. B 94 (2016) 155130.
[43] J. Wen, J. Peng, B. Wang, D.Y. Xing, Phys. Rev. B 75 (2007) 155327;
a Z.Q. Bao, A.M. Guo, Q.F. Sun, J. Phys. Cond. Matter. 26 (2014) 435301.
[44] W.J. Gong, X.Y. Sui, Y. Wang, G.D. Yu, X.H. Chen, Nanoscale Research Lett. 8 (2013) 330;
a W.J. Gong, S.F. Zhang, Z.C. Li, G. Yi, Y.S. Zheng, Phys. Rev. B 89 (2014) 245413.
[45] W. Gong, Y. Zheng, Y. Liu, T. Lü, Phys. Rev. B 73 (2006) 245329.
[46] W.J. Gong, Z. Gao, X.Q. Wang, Curr. Appl. Phys. 15 (2015) 1278.
[47] Y. Okazaki, S. Sasaki, K. Muraki, Phys. Rev. B 84 (2011) 161305(R);
a M. Ferrier, T. Arakawa, T. Hata, R. Fujiwara, R. Delagrange, R. Deblock, Y. Teratani, R. Sakano, A. Oguri, K. Kobayashi, Phys. Rev. Lett. 118 (2017) 196803.

Please cite this article in press as: L.-L. Zhang et al., Transport through a non-Hermitian parallel double-quantum-dot structure in the presence of interdot Coulomb interaction, Superlattices and Microstructures (2017), https://doi.org/10.1016/j.spmi.2017.11.040